Available online at www.sciencedirect.com
ScienceDirect
Journal of Molecular Catalysis A: Chemical 265 (2007) 276–282
JOURNAL OF MOLECULAR CATALYSIS A: CHEMICAL
www.elsevier.com/locate/molcata

Silica supported transition metal-based bimetallic catalysts for vapour phase selective hydrogenation of furfuraldehyde

Benjaram M. Reddy [a,*], Gunugunuri K. Reddy [a], Komateedi N. Rao [a], Ataullah Khan [a], Ibram Ganesh [b]

[a] *Inorganic and Physical Chemistry Division, Indian Institute of Chemical Technology, Uppal Road, Hyderabad 500007, India*
[b] *Ceramic Materials Division, International Advanced Research Centre for Powder Metallurgy and New Materials (ARCI), Balapur, Hyderabad 500005, India*

Received 22 September 2006; received in revised form 16 October 2006; accepted 17 October 2006
Available online 21 October 2006

Abstract

A series of silica supported transition metal-based bimetallic catalysts M–M^1/SiO_2 (M = Co, Ni, and Cu; M^1 = Ni, Cu, and Co) were prepared by deposition precipitation method. Nitrate salts of the corresponding transition metals and colloidal silica were used as precursors. The physicochemical characteristics of the prepared catalysts were investigated by means of X-ray diffraction, thermogravimetry, FT-infrared, scanning electron microscopy-energy dispersive X-ray analysis, and BET surface area techniques. These catalysts were evaluated for selective hydrogenation of furfuraldehyde to furfuryl alcohol in the vapour phase at 423–523 K under normal atmospheric pressure. The XRD measurements reveal formation of a specific solid solution in the case of Cu–Co/SiO_2 and Co–Ni/SiO_2 catalysts. However, in the case of Cu–Ni/SiO_2 catalyst only peaks due to CuO and NiO oxides were observed. The SEM measurements suggest that the prepared bimetallic catalysts are in a highly dispersed form over the surface of the colloidal silica support. Among various catalysts investigated, the Cu–Co/SiO_2 and Ni–Cu/SiO_2 combination catalysts exhibited a high conversion at 523 K and maximum product selectivity at 473 K.

Keywords: Furfuraldehyde; Furfuryl alcohol; Selective hydrogenation; Vapour phase; Bimetallic catalysts; Co–Ni/SiO_2; Ni–Cu/SiO_2; Cu–, Co/SiO_2; Characterization

1. Introduction

Furan chemicals are receiving more significance in recent times because they can be manufactured from renewable sources. Furfuryl alcohol is an important chemical of the furan class compounds mainly produced by hydrogenation of furfural. Furfuryl alcohol is largely used in the production of resins for binding foundry sand to produce cores and molds for metal casting, corrosion resistant mortar for installing acid proof bricks, laminating resins for corrosion resistant fiberglass-reinforced equipment, resins for corrosion resistant furan polymer concrete, impregnating solutions and carbon binders [1,2]. Besides, it is also an important chemical intermediate in the manufacture of lysine, Vitamin C, lubricant, dispersing agent and plastisizer [1,3–5]. Although both vapour and liquid phase hydrogenation of furfural can produce furfuryl alcohol, the vapour phase hydrogenation is usually preferred because it can be carried out at normal atmospheric pressure [3–7]. As a catalyst with moderate activity, copper chromite has been used in the furan industry for the selective hydrogenation of furfural to furfuryl alcohol for decades [1,8,9]. However, the greatest disadvantage associated with this catalyst is its extreme toxicity, which causes severe environmental pollution. Therefore, several attempts could be found in the literature to develop environmentally benign catalysts with different compositions and different preparation methodologies. Some of the reported catalysts include platinum on oxide supports covered with a monolayer of a transition metal oxide [10], Cu/MgO [11], Cu/C [3], Raney Ni [12], amorphous Ni alloys [13,14], Cu–Zn mixed oxides doped with Al, Mn and Fe [15], and homogeneous complexes of Rh, Ru and Pt noble metals [16]. Most of the reported catalysts are sensitive towards sulfur poisoning, relatively expensive and provide moderate product selectivity at high reaction temperatures [17].

* Corresponding author. Tel.: +91 40 27160123; fax: +91 40 27160921.
E-mail addresses: bmreddy@iict.res.in, mreddyb@yahoo.com (B.M. Reddy).

1381-1169/$ – see front matter © 2006 Elsevier B.V. All rights reserved.
doi:10.1016/j.molcata.2006.10.034

Further, all these catalysts produce various side products such as saturated aldehyde, saturated alcohol, 2-methyl furan and other ring opening products. In particular, the high cost of precious metals and the decrease of selectivity at high reaction temperatures have long been motivated the search for better substitute catalysts.

Supported bimetallic catalysts are very interesting materials in general terms since one metal can fine-tune or modify the catalytic properties of the other metal as a result of both structural and electronic effects. Therefore, bimetallic catalysts usually improve both activity and selectivity and even stability of the catalysts [18]. In the field of hydrogenation, bimetallic catalysts are most often used in order to improve selectivity and stability of the single component metal catalysts [19,20]. The catalytic performance of bimetallic catalysts differs significantly from that of the individual components; often show mutual promotion effects towards reduction and increasing thermal stability against sintering [21]. Bimetallic catalysts supported on high specific surface area carriers, such as silica and alumina, have attracted considerable attention recently because of their better performance when compared to the corresponding monometallic counterparts [18]. Additionally, the preparation of supported bimetallic catalysts by different methods could lead to catalysts with new characteristics, where a specific interaction between the two metals could produce a hybrid catalyst whose behavior may differ significantly from that of the catalysts prepared by conventional methods. In the present study, a series of transition metal-based bimetallic M–M^1/SiO_2 (M = Co, Ni, and Cu; M^1 = Ni, Cu, and Co) catalysts have been prepared by a deposition-precipitation method and characterized by various techniques namely, XRD, FT-IR, SEM-EDX and BET surface area methods. The catalytic properties of these materials were evaluated for hydrogenation of furfuraldehyde to furfuryl alcohol in the vapour phase under normal atmospheric pressure.

2. Experimental

2.1. Catalyst preparation

Various bimetallic catalysts M–M^1/SiO_2 (M = Co, Ni, and Cu; M^1 = Ni, Cu, and Co) investigated in this study were prepared by a deposition-precipitation method. Both metals (M–M^1) were deposited over silica support in 1:1 molar ratio (based on metals) keeping the loading amount constant at 20 wt.% with respect to SiO_2. In a typical preparation procedure, the required quantities of the respective metal nitrate salts (Fluka, AR Grade) were dissolved separately in double distilled water and mixed together. To this mixture solution, the required quantity of colloidal silica (40 wt.%, Fluka, AR Grade) was added and the resultant slurry was stirred for 3–4 h to obtain homogeneous mixture. Subsequently, the homogenized slurry was titrated with aqueous ammonia until pH = 8.5. Thus formed precipitated gel was filtered, washed several times until free from anion impurities and dried at 393 K for 16 h. The oven-dried sample was finally calcined at 723 K for 4 h in air atmosphere. A small portion of the finished catalyst was further heated at 873 K for 4 h to evaluate thermal stability.

2.2. Catalyst characterization

Powder X-ray diffraction (XRD) patterns have been recorded on a Siemens D-5000 diffractometer, using Ni-filtered Cu Kα (0.15418 nm) radiation source. Crystalline phases were identified with the help of ASTM Powder Data Files. The BET surface area measurements were made on a Micromeritics Gemini 2360 instrument by N_2 adsorption at liquid nitrogen temperature. Prior to measurements, samples were oven dried at 393 K for 12 h and flushed with argon gas for 2 h. The infrared spectra were recorded on a Nicolet 740 FTIR spectrometer at ambient conditions, using KBr disks with a normal resolution of 4 cm^{-1} and averaging 100 spectra. Scanning electron microscopy analyses were carried out with a Jeol JSM 5410 microscope, operating with an accelerating voltage of 15 kV. Micrographs were taken after coating by gold sputtering. Elemental analysis was carried out on a Kevex, Sigma KS3 EDX instrument operating at a detector resolution of 137 eV.

2.3. Catalyst evaluation

The vapour phase hydrogenation of furfuraldehyde was carried out in a down flow vertical fixed-bed quartz micro-reactor (i.d. 10 mm, length 25 cm) at normal atmospheric pressure. In a typical experiment, ca. 0.25 g of catalyst mixed with twice the amount of quartz powder was secured between two plugs of quartz wool. Ceramic beads were filled above the catalyst bed, which acted as preheating zone. The reactor was placed vertically inside an electrically heated tubular furnace. The reactor temperature was monitored by a K-type thermocouple with its tip located near the catalyst bed. Prior to reaction, the catalyst was pre-reduced in the flow of H_2 for 3 h at 523 K and cooled to reaction temperature. Furfuraldehyde was fed (WHSV ranging from 0.032 to 0.128 mol h^{-1} g $catalyst^{-1}$) from a motorized syringe pump (Perfusor Secura FT, Germany) into the vaporizer where it was allowed to mix uniformly with H_2 gas (20 ml min^{-1}) before entering the preheating zone of the reactor. The liquid products collected through spiral condensers in ice-cooled freezing traps were analyzed by a gas chromatograph using Carbowax packed column and FID detector. The activity data were collected under steady-state conditions. The conversion and product selectivity were calculated as per the procedure described elsewhere [25].

3. Results and discussion

The N_2 BET surface areas of various catalysts prepared in this investigation are shown in Table 1. As can be noted from Table 1, all samples exhibited reasonably high specific surface areas. Among three combinations synthesized, the Cu–Co/SiO_2 sample calcined at 723 K exhibited a high BET surface area of 185 m^2 g^{-1}. The occurrence of high surface areas in the present investigation could be attributed to the employment of colloidal silica support and, also, to the preparation method adopted (deposition–precipitation). The coprecipitation of bimetallic precursors over the colloidal silica is expected to yield smaller crystallites of bimetallic oxides on the surface of the SiO_2 and exhibit a high specific surface area. However, upon calcination

Table 1
Actual metal loadings, metal loadings from EDX analysis, XRD phases observed, and BET SA measurements of various bimetallic M–M^1/SiO_2 (M = Co, Ni, and Cu; M^1 = Ni, Cu, and Co) catalysts calcined at 723 and 873 K

Calcination temperature (K)	BET SA ($m^2\ g^{-1}$)	Actual metal loading (wt.%)		Metal loading from EDX analysis (wt.%)		XRD phases identified
		M	M^1	M	M^1	
Co–Ni/SiO_2						
723	163	10	10	9.8	9.5	$Co_{1.29}Ni_{1.71}O_4$
873	121	–	–	–	–	$Co_{1.29}Ni_{1.71}O_4$
Ni–Cu/SiO_2						
723	161	9.6	10.4	11.1	12.5	NiO; CuO
873	132	–	–	–	–	NiO; CuO
Cu–Co/SiO_2						
723	185	10.38	9.62	11.3	10.4	$Cu_{0.76}Co_{2.24}O_4$
873	159	–	–	–	–	$Cu_{0.76}Co_{2.24}O_4$; CuO

at slightly higher temperature (873 K) a decrease in the surface area is observed (Table 1). This decrease in the surface area is due to sintering of the samples.

The primary objective of employing a support is to achieve an optimal dispersion of the catalytically active components and to stabilize them against sintering. The deposition–precipitation technique takes the advantage of the fact that precipitation onto the preformed carrier needs a lower super saturation than formation of new phases directly from the liquid. The selected support also should be stable under reaction and regeneration conditions and should not adversely interact with the solvent, reactants and reaction products. Therefore, the colloidal silica support has been advantageously employed in the present investigation. The term colloidal silica refers to a stable, dispersion or sols of discrete nanometric particles of amorphous silica, commonly suspended in water with a size of about 7–12 nm in diameter. Depending on the synthesis conditions, the structure of the colloidal particles may differ from isolated spherical particles to agglomerates of complex structures. Colloidal silica exhibits reasonably high specific surface area ranging between 140 and 345 $m^2\ g^{-1}$. The surface area will be typically constant up to the calcination temperatures of 873–973 K. However, the porosity is normally lost at temperatures higher than 1473 K. Since silica is a neutral oxide, there are no strong Brönsted or Lewis acid–base sites on the surface. Untreated silica is totally hydroxylated and the hydroxyl layer is covered with physically adsorbed water [22]. The physically adsorbed water can be removed by treating at 573 K [23]. Thermal treatment of the support leads first to removal of water (dehydration) and then to combination of adjacent hydroxyl groups to form water (dehydroxylation). On silica, the dehydroxylation leads to the formation of surface siloxane bridges [27].

The X-ray powder diffractograms of various samples calcined at 723 and 873 K are shown in Fig. 1. The oxide mixtures that were observed either contained segregated phases of NiO, CuO and CoO or solid solutions of these combinations. Silica normally exists in any of the three crystallographic forms namely, cristobalite, quartz and tridymite. However, no diffraction patterns pertaining to crystalline SiO_2 phase are noted from XRD results. The absence of SiO_2 diffraction patterns indicates that silica is in the amorphous state. In general, the XRD patterns of 723 K calcined samples are relatively broad indicating partly amorphous nature of the samples. The XRD patterns of Co–Ni/SiO_2 sample revealed the presence of a definite compound between cobalt and nickel with the composition $Co_{1.29}Ni_{1.71}O_4$ (JCPDS 40-1191). With increase in calcination temperature from 723 to 873 K, an increase in the intensity of the peaks pertaining to this phase was noted. The increase in the intensity of the peaks is due to better crystallization of the

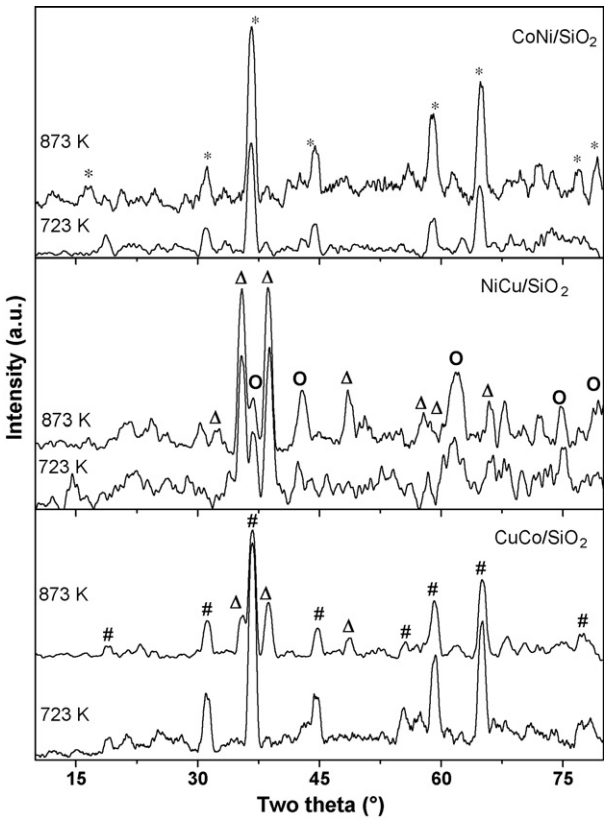

Fig. 1. X-ray diffraction patterns of various bimetallic catalysts M–M^1/SiO_2 (M = Co, Ni and Cu; M^1 = Ni, Cu and Co) calcined at 723 and 873 K; (*) lines due to $Co_{1.29}Ni_{1.71}O_4$ phase; (Δ) lines due to CuO phase; (O) lines due to NiO phase; (#) lines due to $Cu_{0.76}Co_{2.24}O_4$ phase.

sample under the impact of high temperature calcination. The XRD patterns of Ni–Cu/SiO_2 sample revealed the presence of both CuO (JCPDS 48-1548) and NiO (JCPDS 47-1049) phases. With increase in calcination temperature from 723 to 873 K an increase in the intensity of the lines due to better crystallization of these phases was observed. However, as reported by Davies [24], the formation of tetragonal or orthorhombic phases is not found probably due to a different preparation method adopted and the lower calcination temperatures employed in the present study [25]. The XRD profiles of Cu–Co/SiO_2 sample calcined at 723 K revealed the formation of a non-stoichiometric cobalt–copper-oxide solid solution $Cu_{0.76}Co_{2.24}O_4$ (JCPDS 36-1189). This solid solution of general formula $Cu_xCo_{3-x}O_4$ exhibits spinel structure formed by partial migration of copper into the spinel structure of Co_3O_4 compound. Although the standard XRD patterns of $Cu_xCo_{3-x}O_4$ are very similar to that of Co_3O_4, the presence of these Cu–Co oxide solid solutions have been identified in the literature by using the differences in the diffraction patterns from the 311, 511 and 111 planes, corresponding to the differences in d values of around 0.01 Å [26]. Porta et al. [27] investigated Cu- and Co-mixed oxides of different atomic ratios and observed the presence of $Cu_xCo_{3-x}O_4$ and CuO for an atomic ratio of 50:50. They suggested that a change of 0.005 Å in the a_0 cell parameter of the Co_3O_4 phase indicate mixed oxide formation. The formation of a Cu–Co spinel is very difficult and reveals a lower thermal stability [28]. Li et al. [26] synthesized Cu–Co mixed oxides with a Cu/Co atomic ratio of 0.25–1.0 and observed that the Cu–Co spinel is formed above 588 K and stable up to 623 K for Cu/Co < 1. For the sample with Cu/Co = 1, a facile transformation of Cu–Co spinel into CuO and Co_3O_4 was noted. In the present study with increase in calcination temperature from 723 to 873 K, in addition to the existence of $Cu_{0.76}Co_{2.24}O_4$ phase, emergence of a new crystalline CuO phase was noted. This observation is in accordance with the earlier cited literature. With increase in calcination temperature a better crystallization of various phases in the sample is a known phenomenon, which clearly signifies the influence of calcination temperature on the crystallization and formation of new phases in line with literature. It is a reported fact that after reduction and passivation of the Cu–Co solid solution the XRD analysis revealed disappearance of the mixed oxide with the formation of a metallic phase with fcc structure, whose lattice values ($a = b = c = 0.3594$ nm) are intermediate of Cu ($a = 0.3615$ nm) and Co ($a = 0.3545$ nm) metallic phases confirming formation of a Cu–Co alloy system. This was also substantiated by IR spectroscopy [29] of the Cu–Co/Al_2O_3 and transmission electron microscopy of the Cu–Co/SiO_2 [30] catalysts. Therefore, it can be concluded that the alloy formation is favoured by the presence of $Cu_xCo_{3-x}O_4$ phase in the precursor.

The FT-IR spectra of various bimetallic catalysts prepared in this study were recorded in range of 4000–400 cm^{-1}. Normally, strong bands associated with –OH stretching vibrations of water and surface hydroxyl groups occur between 3200 and 3700 cm^{-1}. A sharp and strong absorption band in the region 3650–3700 cm^{-1} was noted in all cases characterizing the presence of hydroxyl groups. Water of hydration usually exhibits one strong band near 3600 cm^{-1} and one or more sharp bands near 3400 cm^{-1}. Water of hydration can be easily distinguished from hydroxyl groups by the presence of the H–O–H bending motion, which produces a medium band in the region 1600–1650 cm^{-1}. Free water has a strong broad absorption band centered in the region 3200–3400 cm^{-1} [31]. Interestingly, all the three bimetallic samples exhibited fairly similar IR patterns, signifying the predominance of silica IR features in the spectra.

To understand the surface morphology and to assess the dispersion of bimetallic active components over the SiO_2 support, SEM investigation was performed on various samples calcined at 723 K. The representative electron micrographs obtained are presented in Fig. 2. The particle size estimation from SEM data reveals that an average particle size in the case of Co–Ni/SiO_2 and Ni–Cu/SiO_2 samples is <10 μm and that of Cu–Co/SiO_2 sample is between 10 and 15 μm. Among the three samples investigated, the Cu–Co/SiO_2 exhibited more porous texture, hence, was also found to exhibit more specific surface area. To get information on the surface composition of the samples, the energy dispersive X-ray microanalysis (EDX) was also performed. As expected, the EDX results revealed the presence of Si, O, Co, Ni and Cu elements in the respective samples in appropriate proportions. The quantitative metal loadings detected (wt.%) in the respective samples are presented in Table 1. For the purpose of comparison the actual metal loadings deposited during the preparation are also shown in Table 1. The EDX results corroborate well, within the limit of permissible error, with the actual metal loadings of the samples.

The catalytic properties of the prepared bimetallic catalysts calcined at 723 K were evaluated for the selective hydrogenation of furfuraldehyde in the vapour phase. As illustrated in Scheme 1, the hydrogenation of furfural(I) is very complex—a well-documented fact in the literature [9]. Besides the main desired product furfuryl alcohol(II), various side products like tetrahydrofurfural(III), tetrahydro furfuryl alcohol(IV), 2-methyl furan(V) and others (1-butanol, 2-pentanone, 2-pentanol, heavy resins—not shown in Scheme 1) could be formed. The formation of furfuryl alcohol and tetrahydrofurfural are parallel reactions, which are competitive, while tetrahydrofurfuryl alcohol is the final product of further hydrogenation of both furfuryl alcohol and tetrahydrofurfural. In the molecule of furfuraldehyde, there is a conjugated system of double bonds on the ring, and a carbonyl double bond that is conjugated with the carbon–carbon double bond as well. If, through modification of the catalyst, the reactivity of the carbonyl double bond relative to that of conjugated carbon–carbon double bonds in the ring were greatly enhanced, the yield of furfuryl alcohol would be highly improved. The activity and selectivity trends for the hydrogenation of furfuraldehyde over various catalysts investigated in the present study at 473 K are depicted in Fig. 3. Interestingly, all these catalysts exhibit a high selectivity towards unsaturated alcohol (furfuryl alcohol) and very small amounts of other byproducts were formed. Recently, Rao et al. [32] reported that Ni-based catalyst exhibits various other hydrogenated products. Also Hao et al. [33] reported formation of 2-methyl furan over Cu–La catalysts. In the present study very less biproducts were observed. The order of the activity for this reaction is as follows: Cu–Co/SiO_2 > Ni–Cu/SiO_2 > Co–Ni/SiO_2. The high

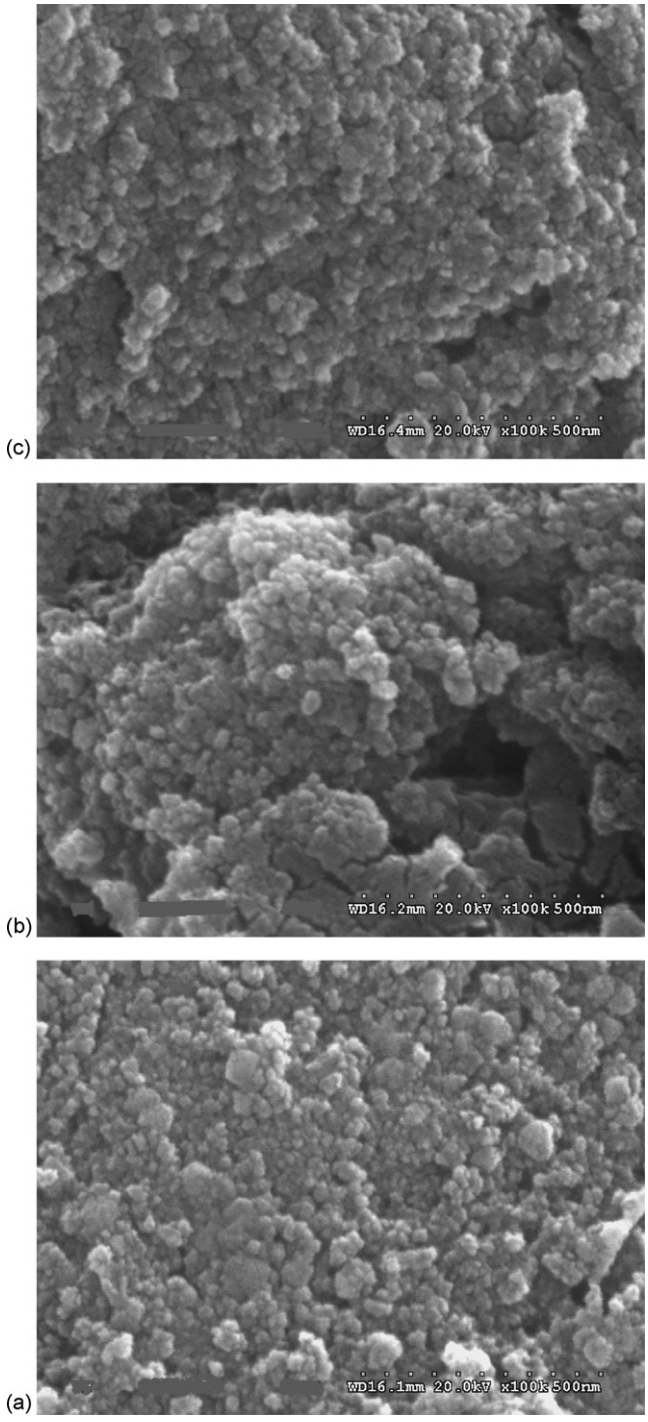

Fig. 2. SEM micrographs of (a) Cu–Co/SiO_2; (b) Ni–Cu/SiO_2; (c) Co–Ni/SiO_2; calcined at 723 K.

activity observed over Cu–Co/SiO_2 catalyst may be due to a high surface area and porous structure of the catalyst as noted from characterization studies.

A series of experiments were conducted to understand the influence of temperature on the conversion and product selectivity of various catalysts. As shown in Fig. 4, the activity profiles obtained in the temperature range 423–523 K follow the same trend with reaction temperature and contact time. In general,

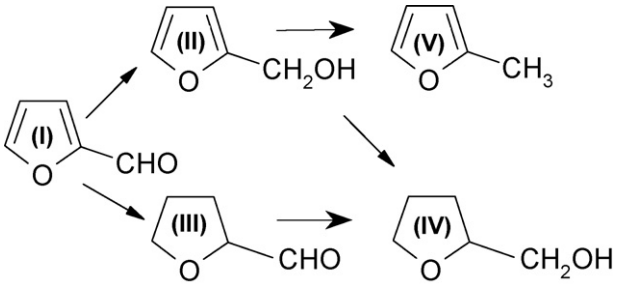

Scheme 1. Reaction scheme of furfuraldehyde hydrogenation.

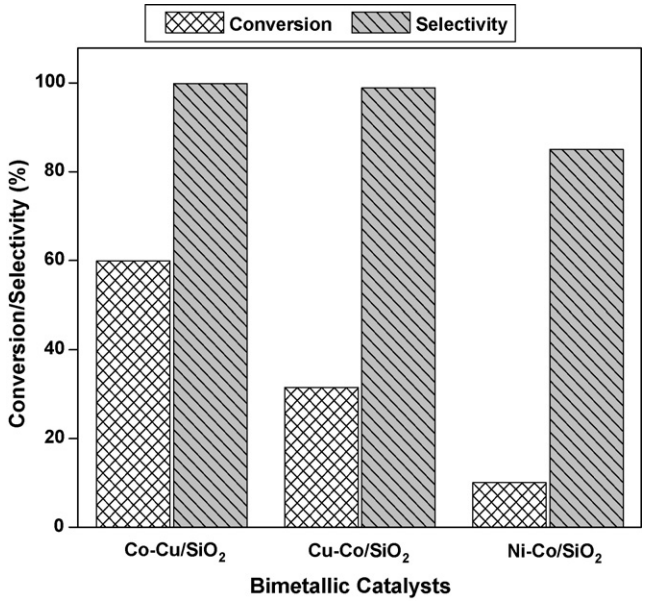

Fig. 3. Conversion and selectivity of various bimetallic catalysts for selective hydrogenation of furfuraldehyde at 473 K.

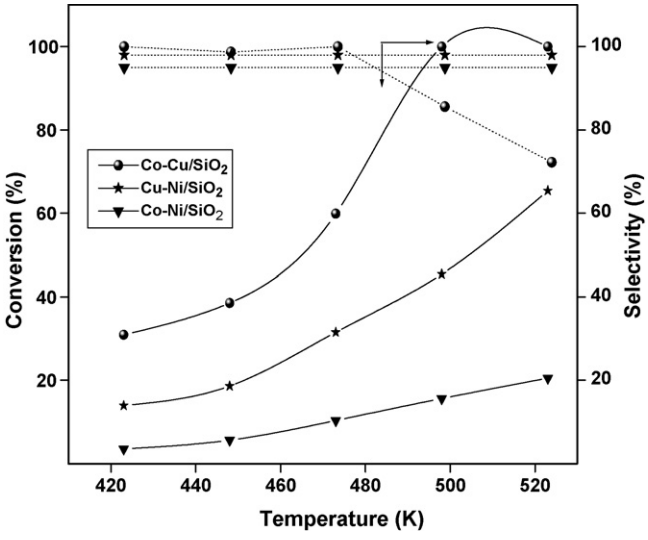

Fig. 4. Temperature vs. activity and selectivity dependence curves of various bimetallic catalysts for selective hydrogenation of furfuraldehyde.

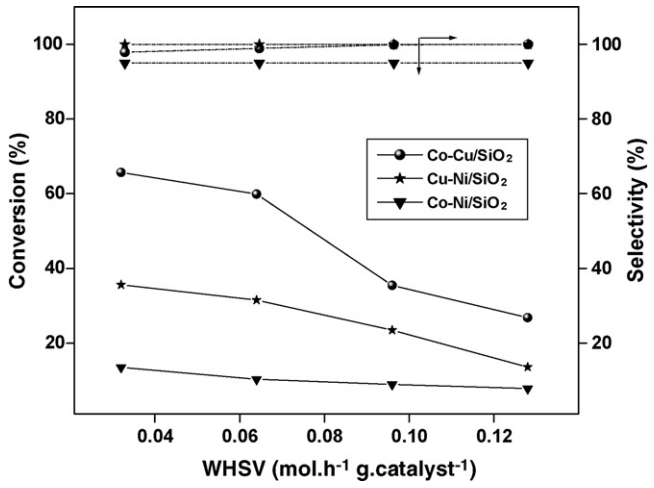

Fig. 5. WHSV of reactant vs. activity and selectivity dependence curves of various bimetallic catalysts for selective hydrogenation of furfuraldehyde at 473 K.

an increase in the conversion with an increase of temperature was observed. The activity was slightly high in the first few minutes and dropped (about 1%) to a level where it remained constant up to the 12 h duration studied. There was no substantial change in the conversion and product selectivity during the 12 h time-on-stream. As stated above the Cu–Co/SiO_2 catalyst exhibited a high conversion at 498 K and above. Interestingly, there is no appreciable change in the selectivity towards furfuryl alcohol with increase of temperature from 423 to 493 K in the case of Cu–Ni/SiO_2 and Co–Ni/SiO_2 catalysts. However, in case of Cu–Co/SiO_2 sample a slight decrease in the selectivity was observed at higher temperatures. The decrease in the selectivity could be due to the occurrence of secondary reactions at high conversion levels as expected. The influence of space velocity on the conversion and selectivity of various catalysts was also investigated at 473 K. Fig. 5 displays the furfuraldehyde conversion and furfuryl alcohol selectivity at different WHSV (mol h^{-1} g $catalyst^{-1}$) ranging from 0.032 to 0.128. As expected the furfuraldehyde conversion decreases with increasing WHSV. The decrease in conversion may be due to shorter contact time of the reactant on the catalyst surface with increasing WHSV. The selectivity remains unchanged with increasing WHSV.

A crucial point in catalytic studies over bimetallic systems is the knowledge of the surface composition of the metallic phase. Experimental studies and theoretical calculations suggest indeed that the surface and bulk composition of alloys may differ, making rather difficult the interpretation of alloying effects on the catalytic activities. In principle, one can vary the surface properties of these catalysts in a systematic manner simply by altering the overall metal composition. The composition of bimetallic catalysts is often significantly different at the surface compared to the bulk due to the differences in surface energies of the two metals. The surface composition or the relative fraction of the two metals at the surface is an important parameter in the study of catalytic phenomena. Further studies will be pursued in that direction over these samples.

4. Conclusions

The following conclusions can be drawn from the present study. The Cu–Co/SiO_2, Ni–Cu/SiO_2 and Co–Ni/SiO_2 bimetallic catalysts exhibit interesting catalytic activity for the vapour phase hydrogenation of furfuraldehyde. (i) The Cu–Co/SiO_2 and Ni–Cu/SiO_2 combination catalysts exhibited a high selectivity towards the formation of furfuryl alcohol. (ii) Incorporation of silica support in the colloidal form during the deposition precipitation of bimetallics resulted in the stable and well-formed catalysts with high specific surface areas. (iii) Further studies are highly essential to investigate the commercial viability of these catalysts for the selective hydrogenation of furfuraldehyde to furfuryl alcohol.

Acknowledgements

GKR and KNR thank University Grants Commission (UGC), New Delhi for the award of junior research fellowships. Financial support received from Department of Science and Technology, New Delhi under SERC Scheme (SR/S1/PC-31/2004).

References

[1] K. Bauer, D. Garbe, Common Fragrance and Flavor Materials, VCH, Kyoto, Japan, 1985.
[2] M.S. Li, W.Z. Ma, Heabi. Ind. (1999) 6.
[3] R.S. Rao, R.T.K. Baker, M.A. Vannice, Catal. Lett. 60 (1999) 51.
[4] De Thomas, US Patent No. 4,153,578 (1979).
[5] F.J. Leo, F.J. Herman, US Patent No. 4,251,396 (1981).
[6] P.A. Elizaveta, M. Juldash, P.P. Ivan, G.G. Lidia, A.G. Jormukhamat, B.A. Ildgam, D.M. Aexei, C.J. Larisa, P.D. Lazar, B.B. Bassheva, US Patent No. 4,261,905 (1981).
[7] F.J. Leo, F.J. Herman, US Patent No. 4,302,397 (1981).
[8] X.-Y. Hao, W. Zhou, J.-W. Wang, Y.-Q. Zhang, S. Liu, Chem. Lett. 34 (2005) 1000.
[9] H. Li, H. Luo, L. Zhuang, W. Dai, M. Qiao, J. Mol. Catal. A: Chem. 203 (2003) 267.
[10] J. Kijenski, P. Winiarek, T. Paryjczak, A. Lewicki, A. Mikoiajska, Appl. Catal. A: Gen. 233 (2002) 171.
[11] B.M. Nagaraja, V.S. Kumar, V. Shasikala, A.H. Padmasri, B. Sreedar, B.D. Raju, K.S.R. Rao, Catal. Commun. 4 (2003) 287.
[12] L. Baijun, L. Lianhai, W. Bingchun, C. Tianxi, K. Iwatani, Appl. Catal. A: Gen. 171 (1998) 117.
[13] S.-P. Lee, Y.-W. Chen, Ind. Eng. Chem. Res. 38 (1999) 2548.
[14] H. Luo, H. Li, L. Zhuang, Chem. Lett. 5 (2001) 404.
[15] J. Nowicki, Z. Maciejewski, Przem. Chem. 76 (1997) 53.
[16] M.J. Burk, T. Gregory, P. Harper, J.R. Lee, Ch. Kalberg, Tetrahedron Lett. 35 (1994) 4963.
[17] V. de Jong, M.K. Cieplik, W.A. Reints, F.-R. Fernandez, R. Louw, J. Catal. 211 (2002) 355.
[18] V. Ponec, Appl. Catal. A: Gen. 222 (2001) 31.
[19] B. Coq, F. Figueras, J. Mol. Catal. A: Chem. 173 (2001) 117.
[20] N. Savargaonkar, B.C. Khanra, M. Pruski, T.S. King, J. Catal. 162 (1996) 277.
[21] G.U. Kulkarni, G. Sankar, C.N.R. Rao, J. Catal. 131 (1991) 491.
[22] D.R. Kinney, I.S. Chuang, G.E. Maciel, J. Am. Chem. Soc. 115 (1993) 6786.
[23] A.A. Tsyganenko, V.N. Filimonov, J. Mol. Struct. 19 (1973) 579.
[24] P.K. Davies, J. Electrochem. Soc. 129 (1982) 31.
[25] B.M. Reddy, I. Ganesh, A. Khan, J. Mol. Catal. A: Chem. 223 (2004) 295.
[26] G.-H. Li, L.-Z. Dai, D.-S. Lu, S.-Y. Peng, J. Solid State Chem. 89 (1990) 167.

[27] P. Porta, R. Dragone, G. Fierro, M. Inversi, M. Lo Jacono, G. Moretti, J. Chem. Soc. Faraday Trans. 86 (1992) 311.
[28] J.L. Gautier, E. Trollund, E. Rios, P. Nkeng, G. Poillerat, J. Electronal. Chem. 428 (1997) 311.
[29] R.M. Bailliard-Letournel, A.J.G. Cobo, C. Mirodotos, M. Primet, A.J. Dalmon, Catal. Lett. 2 (1989) 149.
[30] J.E. Baker, R. Burch, S.J. Hibble, P.K. Loader, Appl. Catal. 65 (1990) 281.
[31] R.A. Nyquist, L.L. Putzig, M.A. Leugers, Handbook of Infrared and Raman Spectra of Inorganic Compounds and Organic Salts, Academic Press, 1997.
[32] R.S. Rao, A. Dandekar, R.T.K. Baker, M.A. Vannice, J. Catal. 171 (1997) 406.
[33] X.-Y. Hao, W. Zhou, J.-W. Wang, Y.-Q. Zhang, S. Liu, Chem. Lett. 34 (2005) 1000.